Geochemical Perspectives Letters

A partial melting control on the Zn isotope composition of basalts

J.M.D. Day, F. Moynier, O. Ishizuka

Supplementary Information

The Supplementary Information includes:

- Methods
- Partial Melting Estimates
- Partial Melting Model
- Table S1
- Figure S1
- Supplementary References

Methods

One hundred and fifty milligram aliquots of powdered boninite and ~30–60 mg of MORB glass were digested in mixtures of ultra-pure 4 parts HF and 1 part HNO_3 in Teflon beakers for 48 hours on a hotplate at 140 °C. Samples were dried down and 6 mol/L ultra-pure HCl was added to dissolve aliquots for another 24 hours at 140 °C on the hotplate. Purification of Zn was achieved using an improved anion-exchange chromatography method, with a recovery of 99.99 % (van Kooten and Moynier, 2019). Samples were loaded in 1.5 mol/L HBr on 0.1 mL AG1-X8 (200–400 mesh) ion-exchange columns with Zn being collected in 0.5 mol/L HNO_3. This step was repeated to purify Zn fractions. A procedural blank measured with samples was 0.2 ng, representing less than 0.1 % of total measured Zn for samples. Isotopic compositions of Zn were measured on the *Thermo Fisher* Neptune Plus multi-collector inductively coupled plasma mass spectrometer (MC-ICP-MS) housed at the Institut de Physique du Globe de Paris. Faraday cups were positioned to collect ions on masses 62, 63, 64, 65, 66, 67 and 68. Possible ^{64}Ni isobaric interferences were corrected by measuring the intensity of the ^{62}Ni peak. A solution containing 10 ppb Zn in 0.1 mol/L HNO_3 was prepared for isotopic analysis. Isotopic ratios of Zn in samples were analysed using an Apex IR introduction system, combined with a 100 L/min PFA nebuliser following van Kooten and Moynier (2019). A single block of 30 ratios, in which the integration time of one scan was 8.3 seconds, was measured for each sample. Background was corrected by subtracting the on-

peak zero intensities from a blank solution. The instrumental mass bias was corrected by bracketing each of the samples with standards. BHVO-2 and AGV-2 gave $\delta^{66}Zn$ = +0.30 ± 0.04 ‰ ($\delta^{68}Zn$ = +0.64 ± 0.06 ‰; 100.2 ppm Zn; n = 4) and $\delta^{66}Zn$ = +0.25 ± 0.08 ‰ ($\delta^{68}Zn$ = +0.53 ± 0.08 ‰; n = 6) respectively, consistent with recommended values (Moynier *et al*., 2017).

Partial Melting Estimates

Based on rare earth element modelling, Shervais *et al*. (2021) demonstrated that boninites form from between ~12 and 23 % partial melting of already refractory harzburgite, dominantly from shallow (spinel stability field) melting. Such high degrees of partial melting are uncommon in the Phanerozoic but were more common in the Archaean where komatiites were generated by as much as 40 ± 10 % partial melting of likely more fertile mantle sources (*e.g.*, Herzberg, 1992). To examine the role of partial melting on Zn isotope fractionation, we compare these extreme endmember rock types with modern mantle-derived basalts from a range of tectonic settings which show a range of MgO contents, Zn abundances and $\delta^{66}Zn$ (Figures 1, S1). Partial melting estimates (Table 2) are conservative estimates of melting, including for MORB (*e.g.*, Asimow *et al.,* 2001), and alkali basalts to nephelinites, the latter of which can be produced by very low degree partial melting of CO_2-bearing lherzolite (*e.g.*, Foley *et al.,* 2009).

Partial Melting Model

Prior workers have developed partial melting models for partial melting of fertile spinel peridotites (Sossi *et al.*, 2018) as well as melting of garnet facies mantle (McCoy-West *et al.*, 2018) and we followed their overall protocol. We developed several partial melting models, using the experimentally determined mineral/melt partitioning for Zn from Davis *et al.* (2013) and utilising melt assemblage starting fractions and melting reactions for spinel peridotite from Wasylenki *et al.* (2003) and garnet peridotite from Walter (1998). We used olivine-orthopyroxene-clinopyroxene-garnet isotope fractionation factors taken from Sossi *et al.* (2018) and McCoy-West *et al.* (2018). Due to the requirement to model both depleted (*i.e.* harzburgitic) and fertile (*i.e.* lherzolitic) partial melting, we used separate model parameters given in Table S1. In addition, we modelled partial melts of metasomatised peridotite. Metasomatised peridotite could vary significantly in modal composition, and we elected to model a composition that only varied cryptically from fertile garnet peridotite, by modifying melting modes and initial starting composition of Zn. We acknowledge that other possibilities exist and could be equally—or more—suitable with our model given solely to exemplify what metasomatism might do for Zn abundances and isotopic compositions in some low degree partial melts.

Supplementary Table

Table S-1 Parameters used in modelling for Figure 2.

Phase	Partitioning	D_{Zn}[a]	$\Delta^{66}Zn$ (‰)[b]	Refractory Mantle		Fertile Mantle		Hybridised Mantle	
				Harz. Starting Fraction[c]	Harz. Melting Reaction[c]	Lherz. Starting Fraction[c]	Lherz. Melting Reaction[c]	MP Starting Fraction[c]	MP Melting Reaction[c]
Olivine	Ol-melt	0.96	$-0.17 \times 10^6/T^2$	0.6	−0.25	0.52	−0.25	0.52	−0.20
Opx	Opx-melt	0.451	$-0.17 \times 10^6/T^2$	0.38	0.35	0.22	0.35	0.22	0.20
Cpx	Cpx-melt	0.333	$-0.17 \times 10^6/T^2$	0	0.8	0.16	0.8	0.16	0.80
Garnet	Grt-melt	0.213	$-0.2 \times 10^6/T^2$	0	–	0.10	0.10	0.10	0.20
Spinel	Sp-melt	5.2	$0 \times 10^6/T^2$	0.02	0.10	0	–	0	–
Initial Zn (ppm) source[d]				40		65		102	
Initial $\delta^{66}Zn$ (‰) source[d]				0.16		0.28		0.42	

[a] Partition coefficients for Zn from Davis *et al.* (2013).

[b] Isotope fractionation factors after work of McCoy-West *et al.* (2018) and Sossi *et al.* (2018).

[c] Starting (modal abundance) fraction and melting reaction values are modified from Walter (1998) and Wasylneki *et al.* (2003).

[d] Initial Zn isotope and abundances for the lherzolite and harzburgite come from average of Doucet *et al.* (2016) data. The metasomatised peridotite (MP) mimicks CL9-078 of Wang *et al.* (2017).

Supplementary Figure

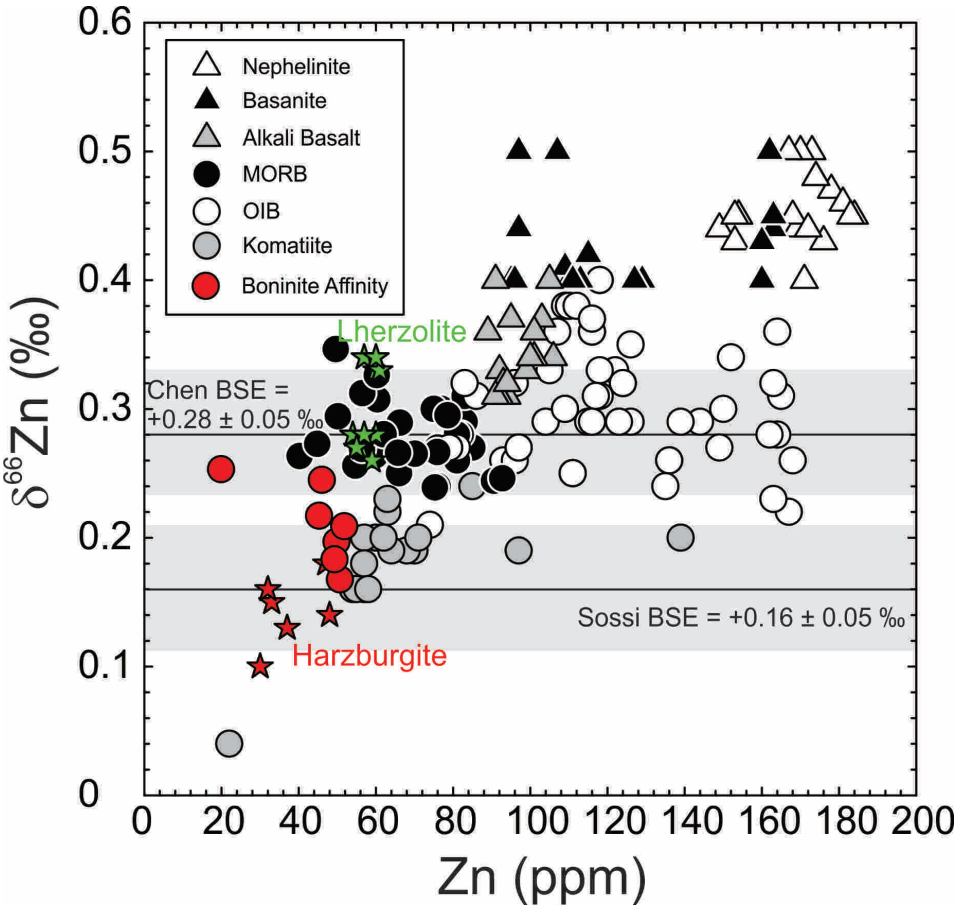

Figure S-1 Zinc isotopic composition as a function Zn abundance for bulk rock samples boninites *versus* low-degree partial melts (nephelinite, basanite, alkali basalt) from Wang *et al.* (2018), mid-ocean ridge basalts (MORB; Wang *et al.*, 2017; this study), ocean island basalts (OIB; Chen *et al.*, 2013; Wang *et al.*, 2017), and komatiites (Sossi *et al.*, 2018) along with fertile lherzolite and depleted harzburgite xenoliths (Doucet *et al.*, 2016). Shown are the estimated bulk silicate Earth (BSE) average (solid line) and standard deviation (shaded regions) values from Chen *et al.* (2013) and Sossi *et al.* (2018).

Supplementary Information References

Asimow, P.D., Hirschmann, M.M., Stolper, E.M. (2001) Calculation of Peridotite Partial Melting from Thermodynamic Models of Minerals and Melts, IV. Adiabatic Decompression and the Composition and Mean Properties of Mid-ocean Ridge Basalts. *Journal of Petrology* 42, 963–998. https://doi.org/10.1093/petrology/42.5.963

Chen, H., Savage, P.S., Teng, F.-Z., Helz, R.T., Moynier, F. (2013) Zinc isotope fractionation during magmatic differentiation and the isotopic composition of the bulk Earth. *Earth and Planetary Science Letters* 369–370, 32–42. https://doi.org/10.1016/j.epsl.2013.02.037

Davis, F.A., Humayun, M., Hirschmann, M.M., Cooper, R.S. (2013) Experimentally determined mineral/melt partitioning of first-row transition elements (FRTE) during partial melting of peridotite at 3 GPa. *Geochimica et Cosmochimica Acta* 104, 232–260. https://doi.org/10.1016/j.gca.2012.11.009

Doucet, L.S., Mattielli, N., Ionov, D.A., Debouge, W., Golovin, A.V. (2016) Zn isotopic heterogeneity in the mantle: A melting control? *Earth and Planetary Science Letters* 451, 232–240. https://doi.org/10.1016/j.epsl.2016.06.040

Foley, S.F., Yaxley, G.M., Rosenthal, A., Buhre, S., Kiseeva, E.S., Rapp, R.P., Jacob, D.E. (2009) The composition of near-solidus melts of peridotite in the presence of CO_2 and H_2O between 40 and 60 kbar. *Lithos* 112, 274–283. https://doi.org/10.1016/j.lithos.2009.03.020

Herzberg, C. (1992) Depth and degree of melting of komatiites. *Journal of Geophysical Research: Solid Earth* 97, 4521–4540. https://doi.org/10.1029/91JB03066

McCoy-West, A.J., Fitton, J.G., Pons, M.L., Inglis, E.C., Williams, H.M. (2018) The Fe and Zn isotope composition of deep mantle source regions: Insights from Baffin Island picrites. *Geochimica et Cosmochimica Acta* 238, 542–562. https://doi.org/10.1016/j.gca.2018.07.021

Moynier, F., Vance, D., Fujii, T., Savage, P. (2017) The Isotope Geochemistry of Zinc and Copper. *Reviews in Mineralogy and Geochemistry* 82, 543–600. https://doi.org/10.2138/rmg.2017.82.13

Shervais, J.W., Reagan, M.K., Godard, M., Prytulak, J., Ryan, J.G., *et al.* (2021) Magmatic Response to Subduction Initiation, Part II: Boninites and Related Rocks of the Izu-Bonin Arc From IODP Expedition 352. *Geochemistry, Geophysics, Geosystems* 22, e2020GC009093. https://doi.org/10.1029/2020GC009093

Sossi, P.A., Nebel, O., O'Neill, H.S.C., Moynier, F. (2018) Zinc isotope composition of the Earth and its behaviour during planetary accretion. *Chemical Geology* 477, 73–84. https://doi.org/10.1016/j.chemgeo.2017.12.006

van Kooten, E., Moynier, F. (2019) Zinc isotope analyses of singularly small samples (<5 ng Zn): Investigating chondrule-matrix complementarity in Leoville. *Geochimica et Cosmochimica Acta* 261, 248–268. https://doi.org/10.1016/j.gca.2019.07.022

Walter, M.J. (1998) Melting of Garnet Peridotite and the Origin of Komatiite and Depleted Lithosphere. *Journal of Petrology* 39, 29–60. https://doi.org/10.1093/petroj/39.1.29

Wang, Z.-Z., Liu, S.-A., Liu, J., Huang, J., Xiao, Y., Chu, Z.-Y., Zhao, X.-M., Tang, L. (2017) Zinc isotope fractionation during mantle melting and constraints on the Zn isotope composition of Earth's upper mantle. *Geochimica et Cosmochimica Acta* 198, 151–167. https://doi.org/10.1016/j.gca.2016.11.014

Wang, Z.-Z., Liu, S.-A., Chen, L.-H., Li, S.-G., Zeng, G. (2018) Compositional transition in natural alkaline lavas through silica-undersaturated melt–lithosphere interaction. *Geology* 46, 771–774. https://doi.org/10.1130/G45145.1

Wasylenki, L.E., Baker, M.B., Kent, A.J.R., Stopler, E.M. (2003) Near-solidus Melting of the Shallow Upper Mantle: Partial Melting Experiments on Depleted Peridotite. *Journal of Petrology* 44, 1163–1191. https://doi.org/10.1093/petrology/44.7.1163